Is the North Indian continental margin a Palaeo-proterozoic magmatic arc? Insights from magnetomineralogy and geochemistry of the Wangtu Gneissic Complex, Himachal Lesser Himalaya

Koushik Sen*, Kavita Tripathi and A. K. Dubey

Wadia Institute of Himalayan Geology, Dehradun 248 001, India

Magnetomineralogical, petrographic and whole-rock geochemical studies on the Palaeo-proterozoic Wangtu Gneissic Complex (WGC) of the Himachal Lesser Himalaya have been carried out to understand the tectonic setting of the northern Indian continental margin during the Palaeo-proterozoic. Petrography and magnetomineralogy suggest that, although the WGC is dominantly composed of S-type/two-mica granitoids having low magnetic susceptibility ($< 500 \times 10^{-6}$ SI units), part of the complex consists of hornblende–magnetite and biotite–magnetite-bearing I-type granitoids having susceptibility greater than 500×10^{-6} SI units. Comparison of magnetic susceptibility with major element concentration reveals that the high susceptibility ($> 500 \times 10^{-6}$ SI units) granites are low in silica content and enriched in ferro-magnesian content. Tectonic discrimination based on trace element concentration shows that both I- and S-type granitoids of the WGC contain concentration of Y, Nb and Rb consistent with a collisional/volcanic arc set up. It is concluded that the North Indian continental margin had an active collisional set up during the Palaeo-proterozoic.

Keywords: Granite, hornblende, Lesser Himalaya, magmatic arc, magnetic susceptibility, proterozoic.

MAGNETIC susceptibility can be used to distinguish between magnetite series and ilmenite series granites[1–4]. Bouchez[5] distinguished paramagnetic and ferromagnetic granites based on their magnetic susceptibility. In general, it is known that granites with high susceptibility ($\geq 1000 \times 10^{-6}$ SI units) have substantial amount of magnetite; they are ferromagnetic and belong to the class of magnetite series granitoids. Paramagnetic or ilmenite series granites have low susceptibility (generally $< 500 \times 10^{-6}$ SI units); their magnetic properties are controlled by paramagnetic minerals like biotite. It is believed that magnetite series granites are formed by mantle-derived magmas and the ilmenite series granites are crustally derived. Aydin *et al.*[6] have shown a strong correlation between concentration of iron oxides in granites with their magnetic susceptibility. They have also suggested that magnetomineralogy of granites can be a good first-order indicator of its geochemical characteristics.

The Wangtu Gneissic Complex (WGC) of the Himachal Himalaya (Figure 1 *a*) is a 1840 ± 16 Ma (zircon U-Pb age)[7] Palaeo-proterozoic gneiss-migmatite complex which is exposed on the footwall of the Vaikrita Thrust (VT)[8] as an antiformal dome, known as the Wangtu Gneissic dome. The complex has undergone deformation and has been transformed into granitic gneiss during the Cenozoic Himalayan orogeny and has been exhumed in late Miocene to Pliocene–Pleistocene[9,10]. The rocks of the WGC are migmatized and mylonitized at some places. Numerous mafic dykes have intruded the WGC. Previous studies have characterized the Palaeo-proterozoic Lesser Himalayan granitic gneisses as S-type granitoids having either a metasedimentary source[11] or having been derived from a pre-existing continental crust[7]. A Palaeo-proterozoic metamorphic event has also been inferred for these granitoids[12]. On the other hand, Kohn *et al.*[13] have suggested a volcanic arc setting for WGC. However, any direct evidence of an active continental tectonic setting in the form of I-type granite magmatism in this area has eluded the workers so far. In the present work, the mineralogical, magnetomineralogical and geochemical aspects of WGC have been studied. This has led to the identification of I-type granite magmatism within WGC, based on which an active arc setting has been suggested for the North Indian continental margin during the Palaeo-proterozoic.

Present study

Petrography

The Wangtu Gneiss is essentially composed of quartz, plagioclase, K-feldspar and biotite along with either mus-

*For correspondence. (e-mail: koushik.geol@gmail.com)

covite or hornblende. Accessory minerals include rutile, zircon, apatite and magnetite. Quartz, plagioclase and K-feldspar are present as megacrysts in a matrix composed of quartz, feldspar, biotite and sometimes hornblende. Based on mineralogy, the WGC can be sub-divided into three types: (1) hornblende–biotite–magnetite-bearing granitoids (Figure 2 *a*–*c*); (2) biotite–magnetite-bearing granitoids and (3) muscovite–biotite-bearing granitoids or two-mica granitoids (Figure 2 *d*). Hornblende and magnetite-bearing granitoids have been further characterized by backscattered electron (BSE) imaging and electron probe micro analysis (EPMA; Figure 2 *c* and Table 1). It is worth noting that EPMA analyses show low TiO_2 content in magnetite and also low total for magnetite (Table 1).

Magnetomineralogy

Five to seven core specimens each were drilled from 19 block samples of WGC. Magnetic susceptibility was measured using KLY-3S Kappabridge at the Wadia Institute of Himalayan Geology (WIHG), Dehdradun. The WGC has been divided into three categories on the basis of magnetic susceptibility: (1) $> 1000 \times 10^{-6}$ SI units, (2) $500–1000 \times 10^{-6}$ SI units and (3) $< 500 \times 10^{-6}$ SI units (Figure 1 *b*; Table 2). The hornblende–biotite–magnetite and biotite–magnetite granitoids have high susceptibility ($> 500 \times 10^{-6}$ SI units) and the two-mica granitoids have low susceptibility ($< 500 \times 10^{-6}$ SI units). Thermomagnetic analysis was carried out for four representative samples, based on their mineralogy and magnetic susceptibility, with a variable field translation balance (MM VFTB, Peterson Instruments). WNG-19 and WNG-24 are low-susceptibility two-mica granitoids, and WNG-20 and WNG-30/2A are high-susceptibility hornblende-bearing granitoids. Temperature variation of magnetization curves of samples WNG-19 and WNG-24 shows dominance of paramagnetic minerals (Figure 3 *a* and *b*). Thermal curves of WNG-20 and WNG-30/2A show a sharp decrease in magnetization at ~580°C (Figure 3 *c* and *d*), indicating the presence of magnetite. These two samples also show a minor ramp at ~350°C. It indicates that the magnetite present in these samples is probably titaniferous.

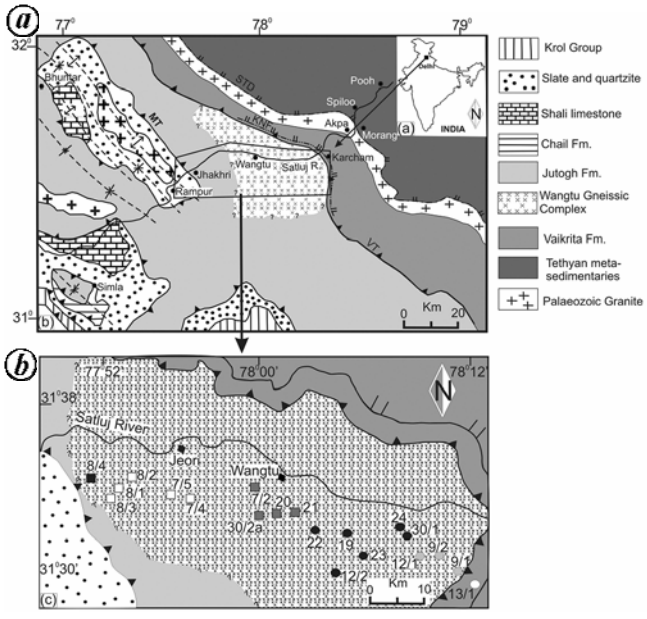

Figure 1. ***a***, Geological map of Himachal Himalaya showing the Wangtu Gneiss and its adjacent lithologies[31]. VT, Vaikrita Thrust; KNF, Karcham Normal Fault; STD, South Tibetan Detachment. ***b***, Sample locations within the Wangtu Gneiss. White circles are samples having magnetic susceptibility $> 1000 \times 10^{-6}$ SI units; grey squares are samples having magnetic susceptibility $> 500 \times 10^{-6}$ SI units and black circles are samples having magnetic susceptibility $< 500 \times 10^{-6}$ SI units.

Major and trace element geochemistry

Major elements were determined using pressed powder pellets by wavelength dispersive X-ray fluorescence (XRF) spectrometry (Siemens SRS 3000). Trace elements were determined using ICP-MS (Perkin-Elmer SCIEX ELAN DRC-e). All geochemical analyses were carried out at WIHG. The precision and accuracy of the preparation and instrumental performance were checked using international reference samples GA, GH, GSN, MA-N (CRPG, France), G-2, GSP-1, RGM-1, AGV-1 (USGS, USA), and JG-2, JG1-a and JA-2 (GSJ, Japan). The accuracy of measurements is <5% for major oxides in XRF and <10% for trace elements in ICP-MS. Precision in terms of maximum observed relative standard deviation on repeated measurements is normally < 2% (ref. 14). Figure 4 shows relationship between major element concentration and mean magnetic susceptibility for all the samples from WGC. The plots show that samples having susceptibility higher than 500×10^{-6} SI units are enriched in MgO, $FeO_{(total)}$ and TiO_2. Samples having susceptibility higher than 500 but lower than 1000×10^{-6} are enriched in CaO and Na_2O. Figure 4 *a* shows a clear negative correlation between silica content and magnetic susceptibility. This is because, with ongoing magmatic differentiation, the granitic melt becomes more felsic and undersaturated in ferro-magnesian content[15]. Mn^{2+} contributes only up to $\sim 6 \pm 2 \times 10^{-6}$ SI units of bulk magnetic susceptibility[6] and therefore does not seem to have much control over the magnetic susceptibility (Figure 4 *i*). Tectonic discrimination diagram based on Y, Nb and Rb concentration[16] was plotted for all the samples (Table 2, Figure 5). Rb versus Nb + Y plots show that all the samples fall near the triple point of fields related to volcanic arc, within plates and collisional granites (Figure 5 *a*). One two-mica granite sample falls in the within-plate field and one sample each from two-mica granite and hornblende–magnetite-bearing I-type granite

Table 1. Electron probe microanalysis (EPMA) data of hornblende and magnetite from sample WNG-23 of the Wangtu Gneiss

Na_2O	MgO	Al_2O_3	SiO_2	P_2O_5	Cr_2O_3	MnO	FeO	CaO	K_2O	TiO_2	Total
Hornblende											
1.39	8.02	11.86	40.99	0.03	0	0.59	19.75	10.08	1.67	0.66	95.04
1.42	8.06	11.61	41.16	0.02	0	0.44	19.45	11.51	1.57	0.62	95.86
1.35	8.04	11.51	40.63	0.02	0.05	0.46	19.69	11.21	1.55	0.55	95.07
1.41	7.75	11.44	40.8	0	0.05	0.49	19.86	11.29	1.54	0.57	95.2
Magnetite											
0.03	0.04	0	0.05	0	0	0.1	88.23	0.04	0	0.03	88.52
0.03	0.03	0	0.04	0	0	0.09	87.52	0.05	0.01	0.03	87.8

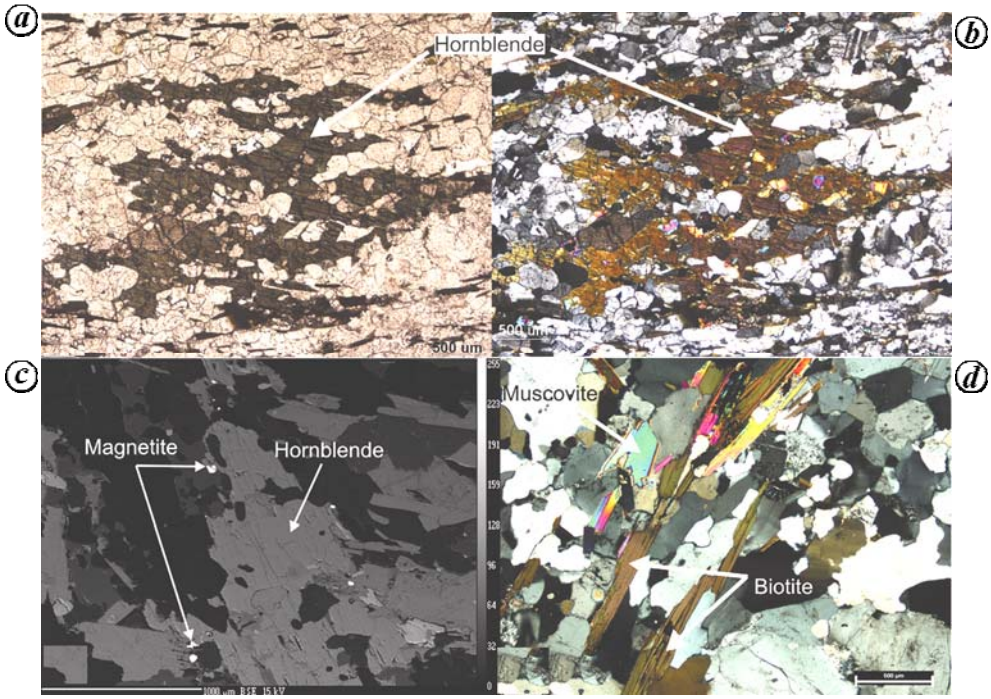

Figure 2. Photomicrographs of the Wangtu Gneiss showing presence of hornblende in (***a***) plane polarized light and (***b***) under cross nicol condition. (***c***) Backscattered electron (BSE) image showing assemblage of hornblende and magnetite, which is typical of I-type granitoids. (***d***) Two-mica variety of granitoids showing presence of both muscovite and biotite.

($> 1000 \times 10^{-6}$ SI units) falls in the volcanic arc field. In case of Nb versus Y plots, few of the two-mica granitoids fall in the within-plate field. All the high-susceptibility granitoids either fall in the volcanic arc/syn-collisional field or close to the line separating collisional and within-plate granites (Figure 5 *b*). Our trace element data negate the possibility of rift origin for any of the granitoids from the WGC.

Discussion

The Proterozoic tectonic set up of the North Indian continental margin has been a matter of conjecture. Whether this margin had been 'active' or 'passive' has significant bearing on the reconstruction of the ~ 1800 Ma Columbia Super continent. Most of the models that were proposed to reconstruct Columbia consider the North Indian continental margin as 'passive', having East Antarctica sandwiched between India and North America[17,18]. On the other hand, Hou *et al.*[19] have suggested a direct contact between India and North America with India's northern margin included along a subduction zone with East Antarctica.

Majority of the earlier workers have inferred the metasedimentary rocks of the lesser Himalaya as a passive margin sedimentary cover[20–23]. Some previous studies carried out in the Proterozoic belt of the Lesser Himalaya have postulated rift or plume model for the felsic and mafic magmatism[24,25]. These are in accordance with the 'passive' model for the North Indian continental margin. On the other hand, detailed geochemical and geochronological study carried out by Kohn *et al.*[13] suggests a

Table 2. Whole-rock major element, trace element and magnetic susceptibility data for samples from the Wangtu Gneiss

Major	Na_2O	MgO	Al_2O_3	SiO_2	P_2O_5	K_2O	CaO	TiO_2	MnO	Fe_2O_3	Sum	Mean magnetic susceptibility (K_m 10^{-6} SI unit) and mineral assemblage
WNG-19	2.85	0.9	14.08	71.18	0.12	5.41	1.75	0.39	0.03	3.42	100.13	150 (two-mica granite)
WNG-24	2.71	1.05	14.29	69.49	0.12	4.5	2.55	0.38	0.03	3.9	99.02	631 (two-mica granite)
WNG-23	2.51	1.81	14.21	67.75	0.17	4.86	2.99	0.43	0.05	4.32	99.1	602 (two-mica granite)
WNG-8/4	2.66	0.37	12.15	74.2	0.07	3.79	1.91	0.38	0.02	3.82	99.37	450 (Bt–Mt-bearing granite)
WNG-8/2	2.45	0.8	13.06	71.35	0.06	5.5	0.98	0.37	0.01	4.17	98.75	123 (two-mica granite)
WNG-12/2	3.12	0.3	13.33	76.05	0.19	5.37	0.47	0.22	0.02	1.81	100.88	48.2 (two-mica granite)
WNG-30/2A	1.44	1.84	14.26	65.94	0.12	3.68	1.11	0.85	0.08	5.81	95.13	1170 (Hbl–Bt–Mt-bearing granite)
WNG-12/1	2.14	0.15	12.3	75.93	0.05	6.02	0.99	0.18	0.02	2.6	100.38	109 (two-mica granite)
WNG-9/1	3.37	0.24	13.07	77.06	0.21	2.39	0.96	0.11	0.06	2.88	100.35	67.4 (two-mica granite)
WNG-8/1	2.56	0.23	12.55	76.01	0.04	5.72	1.26	0.21	0.01	2.8	101.39	154 (two-mica granite)
WNG-8/3	3.14	0.27	12.55	74.65	0.06	4.3	1.39	0.29	0.02	3.54	100.21	168 (two-mica granite)
WNG-30/1	3.4	0.86	14.1	71.4	0.12	4.14	1.75	0.32	0.03	3.83	99.95	757 (Bt–Mt-bearing granite)
WNG-22	3.19	0.53	13.03	75.31	0.09	4.36	1.07	0.34	0.03	2.9	100.85	94.9 (two-mica granite)
WNG-9/2	2.54	0.3	13.95	69.15	0.08	5.89	1.33	0.32	0.03	4.07	97.66	178 (two-mica granite)
WNG-20	2.31	0.99	15.46	65.44	0.16	6.87	2.08	0.55	0.03	3.87	97.76	15600 (Hbl–Bt–Mt-bearing granite)
WNG-7/4	3.01	0.22	13.95	74.23	0.07	6.27	1.09	0.19	0.02	1.76	100.81	92.3 (two-mica granite)
WNG-7/2	2.36	0.84	13.61	69.58	0.14	5.16	1.96	0.54	0.04	3.94	98.17	236 (two-mica granite)
WNG-21	2.97	0.18	13.3	75.1	0.07	6.41	0.73	0.23	0.01	2.13	101.13	370 (two-mica granite)
WNG-7/5	2.46	1.14	14.53	66.16	0.16	5.44	2.22	0.63	0.03	4.58	97.35	1070 (Hbl–Bt–Mt-bearing granite)

Trace	Ba	Cr	V	Sc	Co	Ni	Cu	Zn	Ga	Pb	Th	Rb	U	Sr	Y	Zr	Nb
WNG-19	580	286	28	7.3	9.8	9	5	39	18	44	138	290	23	96	27	299	21
WNG-24	588	315	44	6.9	10.7	13	12	53	18	35	59	268	9.3	207	24	189	16
WNG-23	662	281	62	6.9	14.2	18	9	52	17	35	53	294	14.4	294	26	176	14
WNG-8/2	482	265	26	6.2	11	11	4	26	19	37	112	459	19.3	40	63	340	31
WNG-12/2	214	349	16	4	3.3	7	5	20	18	20	30	328	8.4	18	36	134	21
WNG-30/2A	917	442	102	12	16.3	39	42	73	16	20	16	173	5.3	121	25	244	16
WNG-12/1	609	284	7	4.3	4.9	9	5	33	20	59	125	398	20.8	68	42	209	14
WNG-9/1	233	546	14	5.9	9.1	8	245	36	19	32	81	179	11.8	95	19	81	13
WNG-8/1	706	341	6	5.9	8.4	9	26	21	18	60	146	382	20.9	45	51	353	17
WNG-8/3	548	256	21	7.1	8.2	9	6	38	20	47	145	397	23.9	53	39	338	24
WNG-30/1	546	311	37	7.2	10.3	11	8	40	20	33	59	316	9.9	197	34	183	22
WNG-22	435	257	27	6.6	7.3	8	4	39	19	40	81	327	15.7	67	36	219	24
WNG-9/2	695	130	14	5.9	11.7	8	6	54	20	63	150	426	15.8	62	40	375	21
WNG-20	677	151	45	6.3	9.3	8	7	59	19	40	15	295	5.3	162	33	162	18
WNG-7/4	291	185	9	4.3	3.4	6	7	27	20	57	33	319	9.5	102	37	118	15
WNG-7/2	700	247	41	6.9	10	9	7	55	18	30	36	260	6.6	144	30	226	19
WNG-21	220	233	17	5	5.3	6	9	26	19	65	80	338	8.4	54	35	193	16
WNG-12/1	607	284	8	4.8	5.4	9	5	33	19	59	127	401	19.7	70	42	213	14
WNG-7/5	605	155	53	8.6	10.7	10	21	59	19	30	49	305	9.9	133	35	230	22

Hbl, hornblende; Bt, biotite; Mt, magnetite.

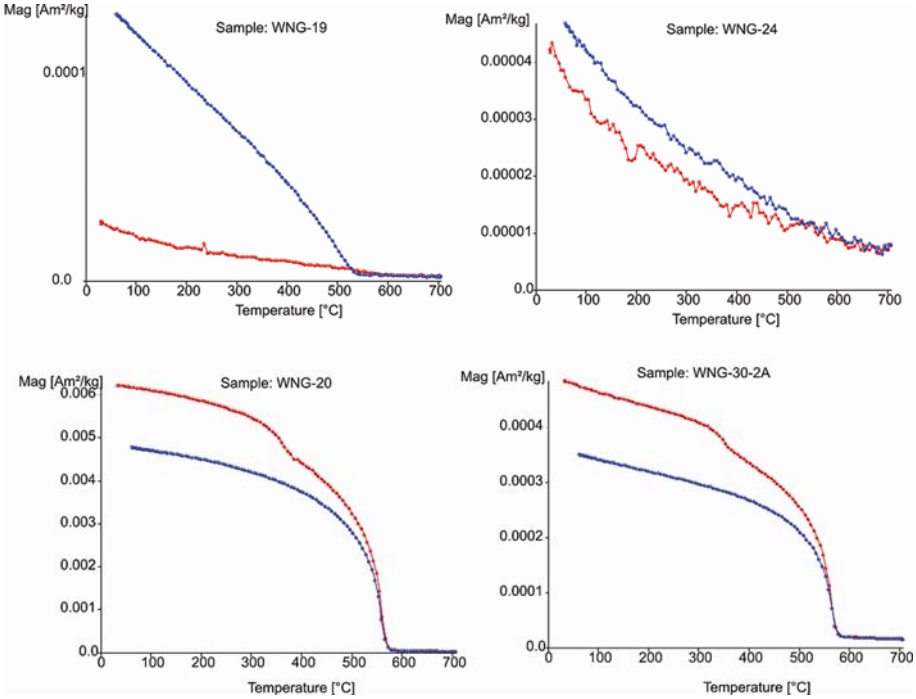

Figure 3. Variation of magnetization with temperature determined for some representative samples of the Wangtu Gneissic Complex (WGC). Samples were selected on the basis of their mean magnetic susceptibility (K_m) and mineralogy. Samples WNG-19 and WNG-24 are low-susceptibility ($< 500 \times 10^{-6}$ SI units) S-type granitoids, and samples WNG-20 and WNG-30/2A are high-susceptibility ($> 1000 \times 10^{-6}$ SI units) hornblende–magnetite-bearing I-type granitoids. Red line is the heating curve and blue line is the cooling curve.

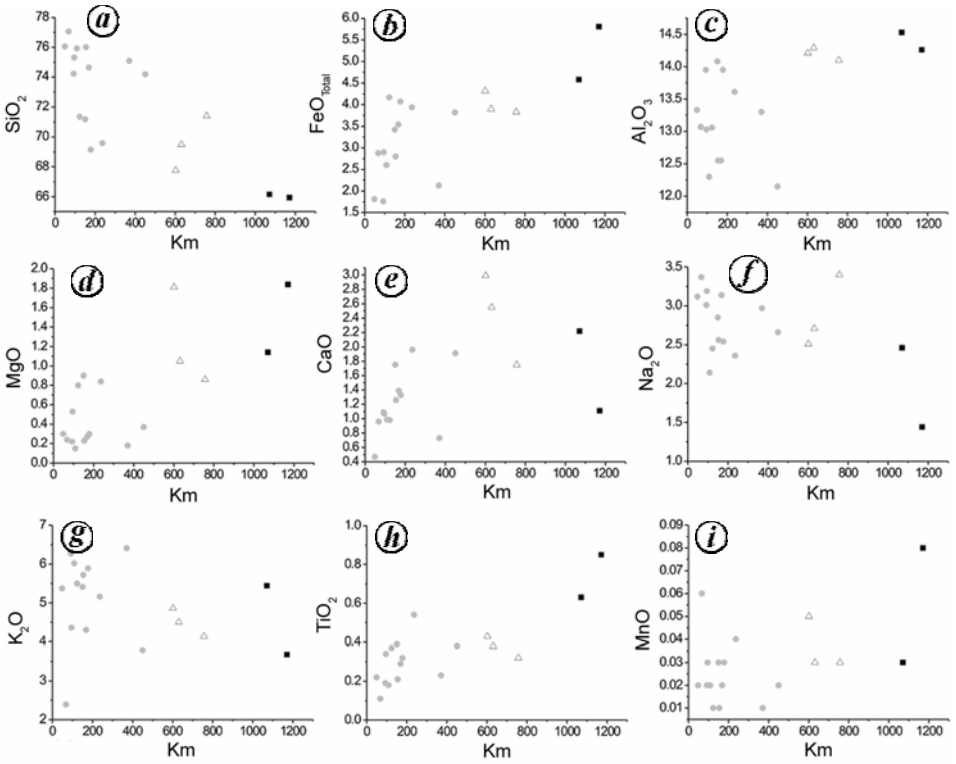

Figure 4. Magnetic susceptibility (K_m) versus SiO_2, FeO_{total}, Al_2O_3, MgO, CaO, Na_2O, K_2O, TiO_2 and MnO (wt%) plots. The number of samples = 18. WNG-20 is excluded in this graph because of its very high range of susceptibility. Black squares are samples having magnetic susceptibility $> 1000 \times 10^{-6}$ SI units; white triangles are samples having magnetic susceptibility $> 500 \times 10^{-6}$ SI units and grey circles are samples having magnetic susceptibility $< 500 \times 10^{-6}$ SI units.

Palaeo-proterozoic arc setting for the North Indian continental margin. Rao and Sharma[26] have inferred that granitoids from the eastern Almora nappe and Chiplakot region of the Kumaun Himalaya were generated through subduction process, and they concluded that the North Indian continental margin was indeed a Palaeo-proterozoic arc.

The Lesser Himalayan Proterozoic granitoids are dominantly S-type two-mica granites and none of the previous studies has reported any mineral assemblage that would suggest an I-type or mantle origin for them. In the present study, three mineralogically distinct facies of granitoids have been identified. Among them, the hornblende, biotite, plagioclase, K-feldspar and quartz granitoids belong to the I-type of Chappell and White[27]. The biotite-bearing granitoids devoid of either hornblende or muscovite characterized by high magnetic susceptibility belong to the magnetite series of granitoids of Ishihara[1]. Their ferromagnetic content also suggests that they are I-type[27,28] (Figure 4). The two-mica granitoids characterized by the presence of both muscovite and biotite belong to S-type of Chappell and White[27]. These granites are devoid of magnetite and are similar to granitoids derived from a crustal/sedimentary protoliths. So from petrographic and magnetomineralogical studies, it can be inferred that some part of WGC is I-type and the rest is S-type. This is further supported by major element geochemical analyses (Table 2). It is shown that samples with higher magnetic susceptibilities are enriched in Fe, Mg and Ti count and are depleted in silica (Figure 4). It is worth mentioning that only five out of 19 samples show I-type affinity and majority of the WGC is S-type. S-type granites are not uncommon in a collisional set up[29]. Trace element geochemistry of WGC indicates that both I- and S-type granitoids of WGC belong to collisional or volcanic arc setting (Figure 5). Kohn *et al.*[13] also found a similar distribution for the Lesser Himalayan granitoids, which fell either in syn-collisional or in volcanic arc fields. Collisional and volcanic arc set up are intimately related in terms of space and time. For example, the Indo-Eurasian collision has caused the Ladakh magmatic arc as well as the Khardung volcanic arc[8]. Earlier studies on WGC have mainly depended on trace element geochemistry to unravel its tectonic setting. Frost *et al.*[30] have suggested that trace element geochemistry of granitoids is more likely to reveal its source and crystallization history rather than tectonic settings. Moreover, trace element analysis can be biased due to crustal contamination (in the present case the Cenozoic Himalayan orogeny), especially for mobile elements like Rb (ref. 13). In view of this, our study presents a direct and reliable evidence of I-type magmatism from the Proterozoic North Indian continental margin through petrographic and magnetomineralogical evidences. The present study clearly suggests that the Proterozoic North Indian continental margin was indeed in a collisional/arc set up and has not remained passive prior to the Himalayan orogeny. I-type granite is rare in the main Himalayan belt. So far only Ladakh granite has been found to be I-type. The I-type granite recognized in WGC, as far as we know, is only the second such occurrence from the main Himalayan mountain belt.

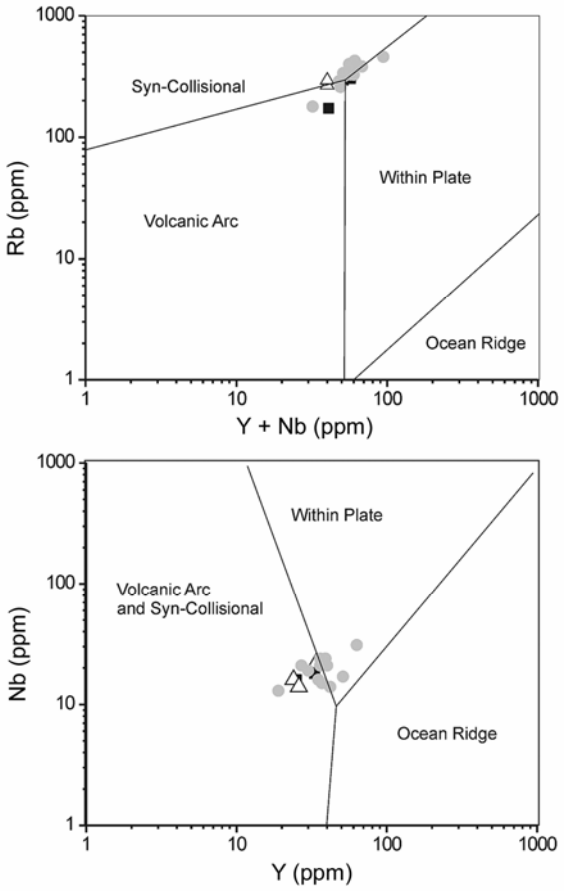

Figure 5. Trace element data (Rb, Y, Nb) plotted on tectonic discrimination diagram[14] showing syn-collisional and volcanic arc affinity of the Wangtu Gneiss. Legends are same as in Figure 4.

1. Ishihara, S., The magnetite-series and ilmenite-series granitic rocks. *Min. Geol.*, 1977, **27**, 293–305.
2. Takahashi, M., Aramaki, S. and Ishihara, S., Magnetite series/ilmenite series vs I-type/S-type granitoids. In *Granitic Magmatism and Related Mineralization* (eds Ishihara, I. and Takenouchi, S.), Mining Geology Nihon Shigen Chishitsu Gakkai–Society of Resource Geologists of Japan, Tokyo, 1980, pp. 13–28.
3. Ellwood, B. B. and Wenner, D. B., Correlation of magnetic susceptibility with $^{18}O:^{16}O$ data in late orogenic granites of the southern Appalachian Piedmont. *Earth Planet. Sci. Lett.*, 1981, **54**, 200–202.
4. Ishihara, S., Hashimoto, M. and Machida, M., Magnetite/ilmenite series classification and magnetic susceptibility of the Mesozoic–Cenozoic batholiths in Peru. *Resour. Geol.*, 2000, **50**, 123–129.
5. Bouchez, J. L., Granite is never isotropic: an introduction to AMS studies of granitic rocks. In *Granite: from Segregation of Melt to Emplacement Fabrics* (eds Bouchez, J. L., Hutton, D. H. W. and Stephens, W. E.), Petrology and Structural Geology, Kluwer, Dordrecht, 1997, vol. 8, pp. 95–112.

6. Aydin, A., Ferré, E. C. and Aslan, Z., The magnetic susceptibility of granitic rocks as a proxy for geochemical composition: example from the Saruhan granitoids, NE Turkey. *Tectonophysics*, 2007, **441**, 85–95.
7. Miller, C., Klötzli, U., Frank, W., Thöni, M. and Grasemann, B., Proteroizoic crustal evolution in the NW Himalaya (India) as recorded by circa 1.80 Ga mafic and 1.84 Ga granitic magmatism. *Precambrian Res.*, 2000, **103**, 191–206.
8. Thakur, V. C., *Geology of Western Himalaya*, Pergamon Press, New York, 1992, p. 363.
9. Jain, A. K., Kumar, D., Singh, S., Kumar, A. and Lal, N., Timing, quantification and tectonic modelling of Pliocene–Quaternary movements in the NW Himalaya: evidence from fission track dating. *Earth Planet. Sci. Lett.*, 2000, **179**, 437–451.
10. Vannay, J. C., Grasemann, B., Rahn, M., Frank, W., Carter, A., Baudraz, V. and Cosca, M., Miocene to Holocene exhumation of metamorphic crustal wedges in the NW Himalaya: evidence for tectonic extrusion coupled to fluvial erosion. *Tectonics*, 2004, **23**, TC 1014; doi: 10.1029/2002TC001429.
11. Sharma, K. K. and Rashid, S. A., Geochemical evolution of peraluminous paleoproterozoic Bandal orthogneiss NW, Himalaya, Himachal Pradesh, India: Implications for the ancient crustal growth in the Himalaya. *J. Asian Earth Sci.*, 2001, **19**, 413–428; doi: 10.1016/S1367-9120(00)00052-3.
12. Pant, N. C., Kundu, A., Kumar, R., Dorka, B. S. and Prasher, S., Palaeo-proterozoic metamorphism in the Jeori–Wangtu Gneissic Crystallines (JWGC), western Himalayas. *J. Asian Earth Sci.*, 2006, **26**, 585–604.
13. Kohn, M. J., Paul, S. K. and Corrie, S. L., The lower Lesser Himalayan sequence: a Palaeo-proterozoic arc on the northern margin of the Indian plate. *Geol. Soc. Am. Bull.*, 2010, **122**, 323–335.
14. Khanna, P. P., Saini, N. K., Mukherjee, P. K. and Purohit, K. K., An appraisal of ICP-MS technique for determination of REEs: long-term QC assessment of silicate rock analysis. *Himalayan Geol.*, 2009, **30**, 95–99.
15. Pitcher, W. S., *The Nature and Origin of Granite*, Blackie Academic and Professional, Glasgow, p. 321.
16. Pearce, J. A., Harris, N. B. W. and Tindle, A. G., Trace element discrimination diagrams for the tectonic interpretation of granitic rocks. *J. Petrol.*, 1984, **25**, 956–983.
17. Rogers, J. J. W. and Santosh, M., Configuration of Columbia, a Mesoproterozoic supercontinent. *Gondwana Res.*, 2002, **5**, 5–22; doi: 10.1016/ S1342-937X(05)70883-2.
18. Zhao, G., Sun, M., Wilde, S. A. and Li, S., A Paleo-Mesoproterozoic supercontinent: assembly, growth and breakup. *Earth-Sci. Rev.*, 2004, **67**, 91–123; doi: 10.1016/j.earscirev.2004.02.003.
19. Hou, G., Santosh, M., Qian, X., Lister, G. S. and Li, J., Configuration of the Late Palaeo-proterozoic super continent Columbia: insights from radiating mafic dyke swarms. *Gondwana Res.*, 2008, **14**, 395–409.
20. Brookfield, M. E., The Himalayan passive margin from Precambrian to Cretaceous times. *Sediment. Geol.*, 1993, **84**, 1–35; doi: 10.1016/0037-0738(93) 90042-4.
21. Upreti, B. N., An overview of the stratigraphy and tectonics of the Nepal Himalaya. *J. Asian Earth Sci.*, 1999, **17**, 577–606; doi: 10.1016/ S1367-9120(99)00047-4.
22. Myrow, P. M. *et al.*, Integrated tectonostratigraphic analysis of the Himalaya and implications for its tectonic reconstruction. *Earth Planet. Sci. Lett.*, 2003, **212**, 433–441; doi: 10.1016/S0012-821X(03)00280-2.
23. Gehrels, G. E., DeCelles, P. G., Ojha, T. P. and Upreti, B. N., Geologic and U–Th–Pb geochronologic evidence for early Paleozoic tectonism in the Kathmandu thrust sheet, central Nepal Himalaya. *Geol. Soc. Am. Bull.*, 2006, **118**, 185–198; doi: 10.1130/ B25753.1.
24. Bhat, M. I., Claesson, S., Dubey, A. K. and Pande, K., Sm–Nd age of the Garhwal–Bhowali volcanics, western Himalayas: vestiges of the Late Archaea Rampur flood basalt province of the northern Indian craton. *Precambrian Res.*, 1998, **87**, 217–231; doi: 10.1016/S0301-9268(97)00076-4.
25. Ahmad, T., Mukherjee, P. K. and Trivedi, J. R., Geochemistry of Precambrian mafic magmatic rocks of the western Himalaya, India: petrogenetic and tectonic implications. *Chem. Geol.*, 1999, **160**, 103–119; doi: 10.1016/S0009-2541(99)00063-7.
26. Rao, D. R. and Sharma, R., Arc magmatism in eastern Kumaun Himalaya: a study based on geochemistry of granitoid rocks. *Island Arc*, 2011, **20**, 500–519.
27. Chappell, B. W. and White, A. J. R., Two contrasting granite types. *Paci. Geol.*, 1974, **8**, 173–174.
28. Chappell, B. W. and White, A. J. R., Two contrasting granite types: 25 years later. *Aust. J. Earth Sci.*, 2001, **48**, 489–499.
29. Sen, K. and Collins, A. S., Dextral transpression and late Eocene magmatism in the trans-Himalayan Ladakh Batholith (North India): implications for tectono-magmatic evolution of the Indo-Eurasian collisional arc. *Int. J. Earth Sci.*, 2012, 1–15; doi: 10.1007/s00531-012-0826-8.
30. Frost, B. R., Barnes, C. G., Collins, W. J., Arculus, R. J., Ellis, D. J. and Frost, C. D., A geochemical classification for granitic rocks. *J. Petrol.*, 2001, **42**, 2033–2048.
31. Thakur, V. C. and Rawat, B. S., *Geological Map of the Western Himalaya*, Wadia Institute of Himalayan Geology, Dehra Dun. scale 1:1,111,111, 1992.

ACKNOWLEDGEMENTS. We thank the Director, WIHG, Dehradun for encouragement and support. We also thank S. S. Thakur for help during fieldwork and P. P. Khanna for help in geochemical analysis. Discussions with Matthew J. Kohn, Rafiqul Islam and B. K. Mukherjee helped improve the manuscript. We also thank the anonymous reviewers for valuable comments.

Received 18 June 2012; revised accepted 3 April 2013